# Hierarchy of modes in an interacting one-dimensional system

Tsyplyatyev, Oleksandr; Schofield, Andrew; Jin, Y; Tan, WK; Ford, CJB; Griffiths, JP; Farrer, I; Jones, GAC; Ritchie, DA

*DOI:*
10.1103/PhysRevLett.114.196401

# Hierarchy of Modes in an Interacting One-Dimensional System

O. Tsyplyatyev and A. J. Schofield
*School of Physics and Astronomy, University of Birmingham, Birmingham B15 2TT, United Kingdom*

Y. Jin, M. Moreno, W. K. Tan, C. J. B. Ford, J. P. Griffiths, I. Farrer, G. A. C. Jones, and D. A. Ritchie
*Cavendish Laboratory, University of Cambridge, J J Thomson Avenue, Cambridge CB3 0HE, United Kingdom*
(Received 13 August 2014; published 11 May 2015)

Studying interacting fermions in one dimension at high energy, we find a hierarchy in the spectral weights of the excitations theoretically, and we observe evidence for second-level excitations experimentally. Diagonalizing a model of fermions (without spin), we show that levels of the hierarchy are separated by powers of $\mathcal{R}^2/L^2$, where $\mathcal{R}$ is a length scale related to interactions and $L$ is the system length. The first-level (strongest) excitations form a mode with parabolic dispersion, like that of a renormalized single particle. The second-level excitations produce a singular power-law line shape to the first-level mode and multiple power laws at the spectral edge. We measure momentum-resolved tunneling of electrons (fermions with spin) from or to a wire formed within a GaAs heterostructure, which shows parabolic dispersion of the first-level mode and well-resolved spin-charge separation at low energy with appreciable interaction strength. We find structure resembling the second-level excitations, which dies away quite rapidly at high momentum.

DOI: 10.1103/PhysRevLett.114.196401 PACS numbers: 71.10.Pm, 03.75.Kk, 73.63.Nm, 73.90.+f

The challenge of understanding interacting electrons is a major open problem. Progress has so far relied on being able to assume a linear relation between energy and momentum that restricts our understanding to the low energy and low momentum excitations where this assumption is valid. This has led to the notion of a Fermi liquid [1] and, in one dimension, a Luttinger liquid [2], where those excitations are described as quasiparticles. In the case of the Luttinger liquid, the quasiparticles are quite distinct from the underlying electrons. In this Letter we have studied a model of interacting fermions where we are not constrained by linearization to low energies and find that the many-body solutions can be characterized in a hierarchical fashion by their "spectral weight"—a quantity determining how the solutions connect to physical observables. At the top of this hierarchy is an excitation that looks like a single underlying fermion but with a new dispersion. We then look for evidence of this hierarchy by undertaking experiments of momentum-conserved tunneling in 1D quantum wires of electrons. We see both the first and second levels of this hierarchy, indicating that this characterization is a robust feature of 1D interacting electrons. Despite its differences from Luttinger-liquid behavior, we are able to show how our hierarchy crosses over to the more familiar Luttinger liquid at low energies.

Our theoretical approach is the full microscopic diagonalization of a model of spinless fermions with short-range interactions and the evaluation of its spectral function via Bethe ansatz methods. We find that the spectral weights of excitations have factors with different powers of a ratio of lengths, $\mathcal{R}^2/L^2$ (which will be defined below) separating them into a hierarchy. The dispersion of the mode formed by excitations with zero power, which we call the first level, is parabolic (see Fig. 1) with a mass renormalized by the Luttinger parameter $K$ [3]. The continuous spectrum of the second-level excitations produces a power-law line shape around the first-level mode with a singular exponent $-1$. Around the hole edge ($h0a$ in Fig. 1) the continuous spectrum reproduces the spectral edge singularity predicted by the very recently proposed mobile impurity model [4],

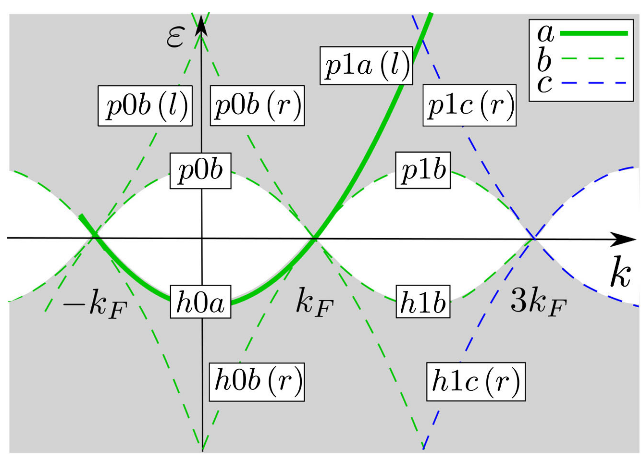


FIG. 1 (color online). The main features of spectral function for spinless fermions in the region $-k_F<k<k_F$ ($k_F<k<3k_F$) labeled by 0(1). The gray areas mark nonzero values, $p(h)$ shows the particle(hole) sector, $k_F$ is the Fermi momentum, $a, b, c$, respectively, identify the level in the hierarchy in powers 0,1,2 of $\mathcal{R}^2/L^2$, and $(r, l)$ specifies the origin in the range—modes on the edge have no such label.

 

but gives a different power-law behavior of the spectral function around the opposite particle edge ($p0b$ in Fig. 1).

Experimentally, we measure the momentum-resolved tunneling of electrons (fermions with spin) confined to a 1D geometry in the top layer of a GaAs-AlGaAs double-quantum-well structure from or to a 2D electron gas in the bottom layer. Probing the spectral function for spinful fermions in this setup we find the same general picture that emerges from the calculation for spinless fermions. We observe a single parabola (which particle-hole asymmetry is manifested in relaxation processes [5]) at high energy, together with well-resolved spin-charge separation (a distinct Luttinger-liquid effect) at low energy with appreciable interaction strength (ratio of charge and spin velocities $v_c/v_s \approx 1.4$) [6,7]. In addition, we can now resolve the structure just above $k_F$ that appears to be the edge of the second-level excitations ($p1b$). However, for higher $k$ we find no sign of the higher-level excitations, implying that their amplitude must have become at least 3 orders of magnitude weaker than for the first parabola ($h0a$). This can only be explained by the hierarchy of modes developed in the theory part of this Letter.

*Spinless fermions.*—We study theoretically the model of interacting Fermi particles without spin in one dimension,

$$H = \int_{-(L/2)}^{L/2} dx \left( -\frac{1}{2m} \psi^\dagger(x) \Delta \psi(x) - UL\rho(x)^2 \right), \quad (1)$$

where the field operators $\psi(x)$ satisfy the Fermi commutation relations, $\{\psi(x), \psi^\dagger(x')\} = \delta(x - x')$, $\rho(x) = \psi^\dagger(x)\psi(x)$ is the particle density operator, and $m$ is the bare mass of a single particle. Below, we consider the periodic boundary condition $\psi(x+L) = \psi(x)$, restrict ourselves to repulsive interaction $U > 0$ only, and take $\hbar = 1$. The response of a many-body system to a single-particle excitation at momentum $k$ and energy $\varepsilon$ is described by a spectral function that, in terms of the eigenstates, reads as [8] $A(k,\varepsilon) = L\sum_f [|\langle f|\psi^\dagger(0)|0\rangle|^2 \delta(\varepsilon - E_f + E_0)\delta(k - P_f) + |\langle 0|\psi(0)|f\rangle|^2 \delta(\varepsilon + E_f - E_0)\delta(k + P_f)]$, where $E_0$ is the energy of the ground state $|0\rangle$, and $P_f$ and $E_f$ are the momenta and the eigenenergies of the eigenstates $|f\rangle$; all eigenstates are assumed normalized.

In the Bethe ansatz approach the model in Eq. (1) is diagonalized by $N$-particle states parametrized with sets of $N$ quasimomenta $k_j$ that satisfy the nonlinear equations $\mathcal{L}k_j - \sum_{l \neq j} \ln[-(e^{i(k_j+k_l)} + 1 - 2mUe^{ik_j})/(e^{i(k_j+k_l)} + 1 - 2mUe^{ik_l})]/i = 2\pi I_j$ [9], where $I_j$ are sets of nonequal integers. The dimensionless length of the system $\mathcal{L} = L/\mathcal{R}$ is normalized by the short length scale $\mathcal{R}$, which is introduced using a lattice (with next-neighbor interaction) as the lattice parameter (and interaction radius) $\mathcal{R}$ that provides microscopically an ultraviolet cutoff for the theory. The latter procedure at high energy is analogous to the point-splitting technique [10] at low energy. Solving the lattice equations in the continuum regime, which corresponds to the thermodynamic ($N, \mathcal{L} \to \infty$, but $N/\mathcal{L}$ is finite) and the long wavelength ($N/\mathcal{L} \ll 1$ with $N/\mathcal{L}$ finite) limits, we obtain [11]

$$k_j = \frac{2\pi I_j}{\mathcal{L} - \frac{mUN}{mU+1}} - \frac{mU}{mU+1} \sum_{l \neq j} \frac{2\pi I_l}{(\mathcal{L} - \frac{mUN}{mU+1})^2}. \quad (2)$$

The corresponding eigenenergy and total momentum (protected by the translational invariance of the system) are $E = \sum_j k_j^2/(2m)$ and $P = \sum_j k_j$. Using the algebraic representation of the Bethe ansatz we obtain the form factor for the spectral function in the same regime as [11,17]

$$|\langle f|\psi^\dagger(0)|0\rangle|^2 = \frac{Z^{2N}}{\mathcal{L}} \frac{\prod_j (k_j^0 - P_f)^2}{\prod_{i,j}(k_j^f - k_i^0)^2} \times \prod_{i<j}(k_j^0 - k_i^0)^2 \prod_{i<j}(k_j^f - k_i^f)^2, \quad (3)$$

where $Z = mU/(mU+1)/[\mathcal{L} - NmU/(1+mU)]$ and $k_j^f$ and $k_j^0$ are the quasimomenta of the eigenstate $|f\rangle$ and the ground state $|0\rangle$.

This result is singular when one or more quasimomenta of an excited state coincide with that of the ground state. The divergences occur in the first term of Eq. (2) but the second (which is smaller in $1/\mathcal{L}$) term provides a cutoff within the theory, canceling a power of $Z^2 \sim \mathcal{L}^{-2}$ per singularity; when $N$ quasimomenta $k_j^f$ coincide with $k_j^0$, Eq. (3) gives $\mathcal{L}|\langle f|\psi^\dagger(0)|0\rangle|^2 = 1$. We label the many-body excitations by the remaining powers of $\mathcal{L}^{-2}$ [18], e.g., $p0b$: $p(h)$ indicates the particle (hole) sector, 0(1) encodes the range of momenta $-k_F < k < k_F$ ($k_F < k < 3k_F$), and $a, b, c$ reflect the terms $\mathcal{L}^{-2n}$ with $n = 0, 1, 2$. All simple modes, formed by single particlelike and holelike excitations of the ground state $k_j^0$, are presented in Fig. 1 and the spectral function along them is evaluated in Table I. Note that the thermodynamic limit involves both $\mathcal{L} \to \infty$ and the particle number $N \to \infty$ and the finite ratio $N/\mathcal{L}$ ensures that the spectral weight of the subleading modes, e.g., the modes $p0b$, $h1b$, and $h1b(r)$, is still apparent in the infinite system.

Excitations around the strongest $a$ modes have an additional electron-hole pair in their quasimomenta, which introduces an extra factor of $\mathcal{L}^{-2}$,

$$|\langle f|\psi^\dagger(0)|0\rangle|^2 = \frac{Z^2}{\mathcal{L}} \frac{(k_2^f - k_1^f)^2 (k_1^0 - P_f)^2}{(k_1^f - k_1^0)^2 (k_2^f - k_1^0)^2}. \quad (4)$$

The energies of the electron-hole pairs themselves are regularly spaced around the Fermi energy with slope $v_F$. However, degeneracy of the many-body excitations due to the spectral linearity makes the level spacings nonequidistant. Using a version of the spectral function smoothed over energy, $\bar{A}(\varepsilon) = \int_{-\epsilon_0/2}^{\epsilon_0/2} d\epsilon A(\varepsilon + \epsilon, k)/\epsilon_0$, where $\epsilon_0$ is a

TABLE I. Spectral weights $A(k, \varepsilon_\alpha(k))$ along the $a$ and the $b$ modes for $-k_F<k<k_F$ ($k_F<k<3k_F$) labeled by $x=0(1)$. Here $\alpha$ is the index of the mode, e.g., $\alpha = h0a$, and other terminology is the same as in Fig. 1; $\gamma = 2\pi/\mathcal{L}$ and $Z = mU/(mU+1)/[\mathcal{L} - NmU/(1+mU)]$.

| | $x=0$ | $x=1$ |
|---|---|---|
| $pxa$ | | 1 |
| $hxa$ | 1 | |
| $pxb$ | $16Z^2k_F^2k^2/(k^2-(k_F+\gamma)^2)^2$ | $4Z^2\gamma^2(k-k_F+\frac{3}{2}\gamma)^2/(k-k_F+\gamma)^2(k-k_F+2\gamma)^2$ |
| $pxb(l)$ | $4Z^2(k_F+k)^2/k_F^2$ | |
| $pxb(r)$ | $4Z^2(k_F-k)^2/k_F^2$ | |
| $hxb$ | | $4Z^2(3k_F-k-\gamma)^2(k_F+k)^2/k_F^2(k-k_F+\gamma)^2$ |
| $hxb(l)$ | $4Z^2\gamma^2/(k+k_F+2\gamma)^2$ | $Z^2k_F^2k^2/((k+\gamma)^2-k_F^2)^2$ |
| $hxb(r)$ | $4Z^2\gamma^2/(k-k_F-2\gamma)^2$ | |

small energy scale, we obtain $\bar{A}(\varepsilon) = Z^2 2k_F(3k^2+k_F^2)/(m\gamma K)(\varepsilon_{h0a}-\varepsilon)^{-1}\theta(\varepsilon_{h0a}-\varepsilon)$ and $\bar{A}(\varepsilon) = Z^2(k+\mathrm{sgn}(\varepsilon-\varepsilon_{p1a(l)})k_F)^3/(m\gamma K)|\varepsilon-\varepsilon_{p1a(l)}|^{-1}$, where $\gamma = 2\pi/\mathcal{L}$ and the dispersion of the $a$ modes is parabolic, $\varepsilon_{h0a}(k) = \varepsilon_{p1a(l)}(k) = k^2/(2mK)$, with the mass renormalized by the Luttinger parameter $K$ [3], around the $h0a$ and $p1a(l)$ modes. The exponent $-1$ coincides with the prediction of the mobile-impurity model [20], where the spectral edge is an $a$ mode, $h0a$.

Excitations around the $b$ modes belong to the same level of hierarchy as the modes themselves, Eq. (4), giving a more complicated shape of the spectral function. Let us focus on one mode, $p0b$. It has a new power-law behavior characterized by an exponent changing with $k$ from $\bar{A}(\varepsilon)\sim(\varepsilon-\varepsilon_{p0b})^3$ for $k=0$ to $\bar{A}(\varepsilon)\sim\mathrm{const}-(\varepsilon-\varepsilon_{p0b})$ for $k\approx k_F$, where $\varepsilon_{p0b}(k) = k_F^2/(mK) - k^2/(2mK)$. This is essentially different from predictions of the mobile-impurity model. Here we observe that the phenomenological model in Refs. [21] is correct only for the $a$-mode spectral edge but higher-order edges require a different field-theoretical description. The density of states is linear, $\nu(\varepsilon)\sim(\varepsilon-\varepsilon_{p0b})$, but level statistics varies from having a regular level spacing (for $k$ commensurate with $k_F$) to an irregular distribution (for incommensurate $k$), which is another microscopic difference between the $a$ and $b$ modes.

Now we use the result in Eq. (3) to calculate another observable, the local density of states. This is independent of position for the translationally invariant systems and, in term of eigenmodes, is [8,22] $\rho(\varepsilon) = \mathcal{L}\sum_f[|\langle f|\psi^\dagger(0)|0\rangle|^2\delta(\varepsilon-E_f+E_0) + |\langle 0|\psi(0)|f\rangle|^2\delta(\varepsilon+E_f-E_0)]$. The leading contribution for $\varepsilon>0$ comes from the $a$ modes, $\rho(\varepsilon) = \theta(\varepsilon)\sqrt{2mK/\varepsilon}$, which gives the same $1/\sqrt{\varepsilon}$ functional dependence as the free-particle model—see red line in Fig. 2. Around the Fermi energy the Tomonaga-Luttinger model predicts power-law suppression of $\rho(\varepsilon)\sim|\varepsilon-\mu|^{(K+K^{-1})/2-1}$ [2] (blue region in Fig. 2) signaling that the leading-order expansion in the $\mathcal{L}|\langle f|\psi^\dagger(0)|0\rangle|^2 = 1$ result is insufficient. We evaluate $\rho(\varepsilon)$ numerically in this region using determinant representation of the form factors for the lattice model instead of Eq. (3) (inset in Fig. 2) [11,23]. Away from the point $\varepsilon=\mu$ the particle-hole symmetry of the Tomonaga-Luttinger model is broken by the curvature of the dispersion of the $a$ modes. For $\varepsilon<0$ the leading contribution to $\rho(\varepsilon)$ comes from $b$ modes. Using Eq. (4) we obtain $\rho(\varepsilon) = 2Z^2k_F^2/(\gamma\mu K)[2(1-3|\varepsilon|/\mu)\sqrt{\mu}\cot^{-1}(\sqrt{|\varepsilon|/\mu})/\sqrt{|\varepsilon|}+6]\theta(-\varepsilon)$, which contains another van Hove singularity $\rho(\varepsilon) = 2\pi Z^2k_F^2/(\gamma K\sqrt{\mu\varepsilon})$ at the bottom the conduction band (green line in Fig. 2).

Having established the theoretical framework for expecting a hierarchy of modes in our calculation, we now turn to experiment and the evidence from momentum-conserving tunneling of electrons. Electrons, being spin-1/2, do not directly correspond to the model above (and neither is there a method known for calculating the necessary form factors for spinful fermions). Nevertheless, the general picture that emerges for the experiment is qualitatively the same as we have established theoretically above and it provides additional support for the existence of a hierarchy.

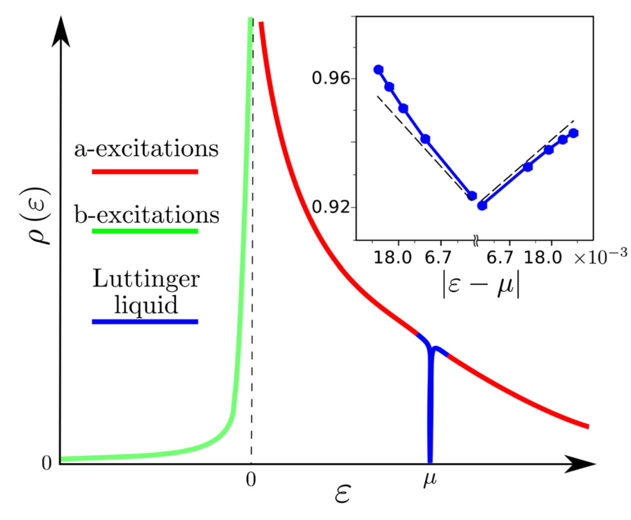


FIG. 2 (color online). The local density of states for spinless fermions: red and green lines show the contribution of $a$ and $b$ excitations and the blue line indicates the Luttinger-liquid regime. Inset is a log-log plot around the Fermi energy: the blue points are numerical data for $N=71$, $L=700$, $mV=6$ giving $K=0.843$, and the dashed line is $\rho(\varepsilon) = \mathrm{const}|\varepsilon-\mu|^{(K+K^{-1})/2-1}$.

*Fermions with spin.*— We study experimentally in a high-mobility GaAs-AlGaAs double-quantum-well structure with electron density around $2\times10^{15}$ m$^{-2}$ in each layer. Electrons in the top layer are confined to a 1D geometry by split gates. Our devices contain an array of ~500 highly regular wires to boost the signal from 1D to 2D tunneling. The small lithographic width of the wires, ~0.18 $\mu$m, provides a large energy spacing between the first and second 1D subbands, allowing a wide energy window for electronic excitations in the single-subband case—see device schematic in Fig. 3(f) and more details in Ref. [7].

The 2DEG in the bottom layer is separated from the wires by a $d = 14$ nm tunnel barrier (giving a spacing between the centers of the wave functions of $d = 34$ nm). It is used as a controllable injector or collector of electrons for the 1D system [24]. A sharp spectral feature in the density of states of the 2DEG produced by integration over momenta in the direction perpendicular to the wires can be shifted in energy by a dc bias between the layers, in order to probe different energies. Also, an in-plane magnetic field $B$ applied perpendicular to the wires changes the longitudinal momentum in the tunneling between layers by $\Delta k = eBd/\hbar$, where $e$ is the electronic charge, and so probes the momentum. Together they reveal the dispersion relation of states in each layer. In this magnetic field range the system is still within the regime of Pauli paramagnetism for the electron densities in our samples.

We have measured the tunneling conductance $G$ between the two layers [see Fig. 3(f)] in detail in a wide range of voltage and magnetic field, corresponding to a large portion of the 1D spectral function from $-k_F$ to $3k_F$ and from $-2\mu$ to $2\mu$ [Fig. 3(a)]. At low energy we observe spin-charge separation [7]. The slopes of the charge ($C$) and spin ($S$) branches—black dashed lines—are $v_c \approx 2.03\times10^5$ and $v_s \approx 1.44\times10^5$ ms$^{-1}$, respectively, with $v_c/v_s \approx 1.4\pm0.1$ [11]. This large ratio, together with a strong zero-bias suppression of tunneling [7], confirms that our system is in the strongly interacting regime.

Unavoidable “parasitic” ($p$’) tunneling from narrow 2D regions connecting the wires to the space constriction [7], superimpose a set of parabolic dispersions, marked by magenta and blue dotted lines in Fig. 3(a) on top of the 1D to 2D signal. Apart from them we observe a 1D parabola, marked by the solid green line in Fig. 3(a), which extends from the spin-excitation branch at low energy. The position of its minimum gives the 1D chemical potential $\mu \approx 3$ meV and its crossings with the line $V_{\mathrm{dc}} = 0$, corresponding to momenta $-k_F$ and $k_F$, give the 1D Fermi momentum $k_F \approx 8\times10^7$ m$^{-1}$.

All other edges of the 1D spectral function are constructed by mirroring and translation of the hole part of the observable 1D dispersion, the dashed green and blue lines in Fig. 3. We observe a distinctive feature in the region just above the higher $V_{\mathrm{dc}} = 0$ crossing point ($k_F$): the 1D peak, instead of just continuing along the noninteracting

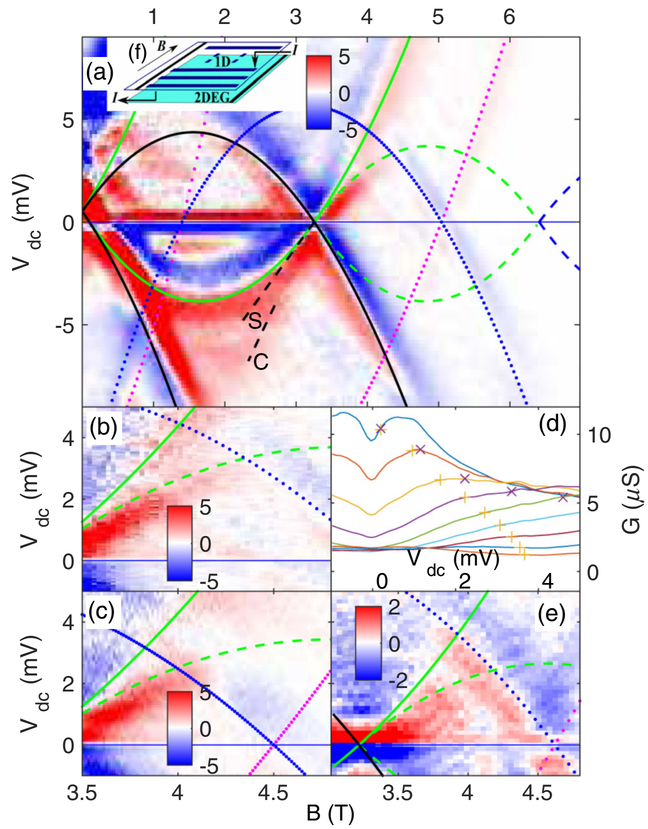


FIG. 3 (color online). Measurement of the tunneling differential conductance $G = dI/dV$ for two samples, each consisting of a set of identical wires of length $L = 10$ (a)–(d) and $L = 18$ $\mu$m (e), sketched in inset (f). (a) Intensity plot of $dG/dV_{\mathrm{dc}}$ to $2\mu$. The line is the 2D dispersion. The green solid line marks the $a$ modes, dashed green lines the $b$ modes, and dashed blue the $c$ modes (as in Fig. 1); dotted magenta and blue lines are parasitic 2D dispersions. Spin ($S$) and charge ($C$) modes are indicated with black dashed lines. $T = 300$ mK. (b) Enlargement of the replica feature in (a) just above $k_{\mathrm{F}}$. It appears as a pale band (slowly varying $G$) between the two green curves, after a red region (sharp rise in $G$). (c) The same as in (b), but with the gate voltage over most of the parasitic ($p$’) region changed to move the $p$’ parabolas. (d) $G$ vs $V_{\mathrm{dc}}$ at various fields $B$ from 3 to 4.8 T [from (a)]; $+$ and $\times$ symbols on each curve indicate, respectively, the voltages corresponding to the dashed and solid [$p1b$ and $p1a(l)$] green lines in (a) and (b), showing the enhanced conductance between the two. (e) $dG/dV_{\mathrm{dc}}$ for a second device, at $T<100$ mK. The replica feature is similar to that shown in (b) and (c) for the other sample.

parabola, broadens, with one boundary following the parabola [$p1a(l)$] and the other bending around, analogous to the replica $p1b$. This is observed in samples with different wire designs and lengths [10 (a)–(d), and 18 $\mu$m (e)] and at temperatures from 100 up to at least 300 mK. The strength of the $p1b$ feature decreases as the $B$ field increases away from the crossing point analogously to that for spinless fermions in Table I [25], though it then passes a $p$’ parabola. (b) and (c) show the replica feature [26] for two different positions of the $p$’ parabolas using a gate above most of the $p$' region, showing that the replica feature is independent of the $p$' tunneling. $G$ is plotted in (d) on cuts along the $V_{\mathrm{dc}}$ axis of (a) at various fields $B$ from 3 to 4.8 T; between the $+$ and $\times$ symbols on each curve is the region of enhanced conductance, characteristic of the replica $p1b$. The amplitude of the feature dies away rapidly, and beyond the $p$' parabolas, we have measured up to 8 T with high sensitivity, and find no measurable sign of any feature above the experimental noise threshold. This places an upper limit on the amplitude of any replica away from $k_F$ of at least 3 orders of magnitude less than that of the $a$ mode ($h0a$).

Making an analogy with the microscopic theory for spinless fermions above, we estimate the ratio of signals around different spectral edges using the 1D Fermi wavelength, $\lambda_F \approx 80$ nm for our samples, as the short-range scale. The amplitude of signal from the second (third)-level excitations is predicted to be smaller by a factor of more than $\lambda_F^2/L^2 = 6\times10^{-5}$ ($\lambda_F^4/L^4 = 4\times10^{-9}$), where the length of a wire is $L = 10$ $\mu$m. These values are at least an order of magnitude smaller than the noise level of our experiment. Thus, our observations are consistent with the mode hierarchy picture for fermions.

In conclusion, we have shown that a hierarchy of modes can emerge in an interacting 1D system controlled by the system length. The dominant mode for long systems has a parabolic dispersion, like that of a renormalized free particle, in contrast with distinctly nonfreeparticle-like behavior at low energy governed by the Tomonaga-Luttinger model. Experimentally, we find a clear feature resembling the second-level excitations, which dies away at high momentum.

We acknowledge financial support from the UK EPSRC through Grants No. EP/J01690X/1 and No. EP/J016888/1.

[1] P. Nozieres, *Theory of Interacting Fermi Systems* (Addison-Wesley, Reading, MA, 1997).
[2] T. Giamarchi, *Quantum Physics in One Dimension* (Clarendon Press, Oxford, 2003).
[3] O. Tsyplyatyev and A. J. Schofield, Phys. Rev. B **90**, 014309 (2014).
[4] A. Imambekov, T. L. Schmidt, and L. I. Glazman, Rev. Mod. Phys. **84**, 1253 (2012).
[5] G. Barak, H. Steinberg, L. N. Pfeiffer, K. W. West, L. Glazman, F. von Oppen, and A. Yacoby, Nat. Phys. **6**, 489 (2010).
[6] O. M. Auslaender, A. Yacoby, R. de Picciotto, K. W. Baldwin, L. N. Pfeiffer, and K. W. West, Science **295**, 825 (2002).
[7] Y. Jompol, C. J. B. Ford, J. P. Griffiths, I. Farrer, G. A. C. Jones, D. Anderson, D. A. Ritchie, T. W. Silk, and A. J. Schofield, Science **325**, 597 (2009).
[8] A. A. Abrikosov, L. P. Gorkov, and I. E. Dzyaloshinski, *Methods of Quantum Field Theory in Statistical Physics* (Dover, New York, 1975).
[9] V. E. Korepin, N. M. Bogoliubov, and A. G. Izergin, *Quantum Inverse Scattering Methods and Correlation Functions* (Cambridge University Press, Cambridge, England, 1993).
[10] J. von Delft and H. Schoeller, Ann. Phys. (N.Y.) **7**, 225 (1998).
[11] See Supplemental Material at http://link.aps.org/supplemental/10.1103/PhysRevLett.114.196401, which includes Refs. [12–16], and at the Universities of Cambridge and of Birmingham data repositories at http://www.repository.cam.ac.uk/handle/1810/247433 and http://epapers.bham.ac.uk/1956/.
[12] M. Gaudin, B. M. McCoy, and T. T. Wu, Phys. Rev. D **23**, 417 (1981); V. E. Korepin, Commun. Math. Phys. **86**, 391 (1982).
[13] N. Kitanine, J. M. Maillet, and V. Tetras, Nucl. Phys. **B554**, 647 (1999); Nucl. Phys. **B567**, 554 (2000).
[14] N. A. Slavnov, Theor. Math. Phys. **79**, 502 (1989).
[15] V. G. Drinfeld, DOKLADY AKADEMII NAUK SSSR **273**, 531 (1983) [Sov. Math. Dokl. **28**, 667 (1983)].
[16] F. Gohmann and V. E. Korepin, J. Phys. A **33**. 1199 (2000); K. Motegi and K. Sakai, Nucl. Phys. **B793**, 451 (2008).
[17] The result in Eq. (3) was verified by direct summation over spatial variables for up to $N = 3$ particles.
[18] A similar hierarchy of excitations is observed in numerical studies of spin chains at large fillings, e.g., Ref. [19], for which Eq. (3) is not applicable.
[19] J.-S. Caux and J. M. Maillet, Phys. Rev. Lett. **95**, 077201 (2005).
[20] O. Tsyplyatyev and A. J. Schofield, Phys. Rev. B **88**, 115142 (2013).
[21] M. Pustilnik, M. Khodas, A. Kamenev, and L. I. Glazman, Phys. Rev. Lett. **96**, 196405 (2006); A. Imambekov and L. I. Glazman, Phys. Rev. Lett. **102**, 126405 (2009).
[22] This is equivalent to the conventional definition, $\rho(x,\varepsilon) = -\mathrm{Im}[\int dt e^{-i\varepsilon t} G(x,x,t)]\mathrm{sgn}(\varepsilon-\mu)/\pi$, using the two point correlation function $G(x,x',t) = -i\langle T[e^{-iHt}\psi(x)e^{iHt}\psi^\dagger(x')]\rangle$ at zero temperature.
[23] The regions of validity of the Tomonaga-Luttinger model and Eq. (3) have a large overlap around $\varepsilon = \mu$ since power-law suppression of $\rho(\varepsilon)$ has a very small exponent due to only small deviations from $K = 1$ for arbitrary short-range interactions between spinless fermions.
[24] A. Altland, C. H. W. Barnes, F. W. J. Hekking, and A. J. Schofield, Phys. Rev. Lett. **83**, 1203 (1999).
[25] From Table I for spinless fermions it is natural to expect that divergence of the spectral weight of a $b$ mode toward an $a$ mode is a general feature, but there is no known method for performing a microscopic calculation in the spinful case.
[26] The $h0b(r)$ mode should (from Table I) be comparable to $p1b$ but it would be very difficult to resolve it due to the overlaying spin and charge lines.